Smart IoT-Based Solar Charger Management System for Optimizing Clean and Affordable Energy Consumption

Muhammad Akbar Pratama Putra[1]*, Bryan Louis Sutanto[2], Michael Kurniawan Santosa[3], Bayu Saputra[4], Gholi Kukuh Mustari[5]

[1]*Department of Physics, Faculty of Mathematics and Natural Sciences, Universitas Negeri Jakarta, Indonesia*
[2]*Department of Physics, Faculty of Mathematics and Natural Sciences, Universitas Negeri Jakarta, Indonesia*
[3]*Department of Public Sector Accounting, Faculty of Economics and Business, Universitas Negeri Jakarta, Indonesia*
[4]*Department of Electronic Engineering Education, Faculty of Engineering, Universitas Negeri Jakarta, Indonesia*
[5]*Department of Electrical Engineering Education, Faculty of Engineering, Universitas Negeri Jakarta, Indonesia*

ABSTRACT

The rapid growth of energy consumption and environmental concerns require sustainable renewable technologies, particularly solar energy. However, inefficient energy management often limits its effectiveness. This study proposes an IoT-based Smart Solar Energy Management System to optimize energy generation, storage, and consumption in real time. The system integrates solar panels, battery storage, sensors, microcontrollers, and IoT communication to monitor parameters and distribute energy efficiently. Using an ESP32 microcontroller and calibrated INA219 sensors, the prototype automates overcharge protection via an electromechanical relay and hysteresis control. Experimental results demonstrate high measurement accuracy with over 99% current error reduction, rapid cut-off response times, and robust Telegram telemetry with a 100% packet delivery success rate. The system ensures thermal stability and reliable operation under field conditions. By providing an affordable and accessible smart energy management tool, this innovation directly supports Sustainable Development Goal (SDG) 7 in enhancing clean, reliable, and sustainable energy availability for communities.

ABSTRAK

Pesatnya pertumbuhan konsumsi energi serta peningkatan isu lingkungan mendorong kebutuhan teknologi energi terbarukan yang berkelanjutan, khususnya energi surya. Namun, pengelolaan yang kurang efisien sering kali membatasi efektivitasnya. Penelitian ini mengusulkan pengembangan Smart Solar Energy Management System berbasis Internet of Things (IoT) untuk mengoptimalkan pembangkitan, penyimpanan, dan konsumsi energi secara real-time. Sistem ini mengintegrasikan panel surya, baterai, sensor, mikrokontroler, dan komunikasi IoT guna memantau parameter kelistrikan serta mendistribusikan daya secara efisien. Menggunakan mikrokontroler ESP32 dan sensor INA219 terkalibrasi, prototipe ini mengotomatisasi proteksi pengisian berlebih melalui relay elektromekanis dan kontrol histeresis. Hasil eksperimen menunjukkan akurasi pengukuran yang tinggi dengan reduksi kesalahan arus di atas 99%, respons pemutusan yang cepat, serta telemetri Telegram yang andal dengan tingkat keberhasilan pengiriman paket 100%. Sistem ini juga memastikan stabilitas termal dan operasional yang optimal. Melalui penyediaan manajemen energi cerdas yang terjangkau, inovasi ini mendukung pencapaian Sustainable Development Goal (SDG) 7 dalam penyediaan energi bersih dan berkelanjutan.

CONTACT

muhammad.akbar.pratama01@mhs.unj.ac.id

KEYWORDS

Internet of Things (IoT), Smart Energy Management System, Solar Energy

Received: 24/08/2026
Revised: 22/10/2026
Accepted: 27/10/2026
Online: 31/10/2026
Published: 31/10/2026

JoC is licenced under a Creative Commons Attribution 4.0 International Public Licence (CC-BY 4.0)

10.21009/joc.13.05

INTRODUCTION

The demand for electrical energy across Indonesia has escalated markedly over the past decade, driven by accelerated industrialization, expanding commercial activities, and rising residential standards of living. According to official data from the Ministry of Energy and Mineral Resources (ESDM, 2024), national electricity consumption reached 1,337 kWh/capita in 2023, representing an annual increase of 13.98% over the 2022 level of 1,173 kWh/capita. Despite this substantial growth, nationwide electrification parity remains incomplete, particularly across remote archipelagos, isolated rural settlements, and mountainous topographies where centralized grid extension is economically and geographically prohibitive (Wijaya *et al.*, 2021). Remote communities frequently endure severe power reliability deficits, highlighting an urgent imperative for decentralized, independent, and sustainable microgrid solutions leveraging local renewable energy resources (Nasir *et al.*, 2020; Sivaprakasam *et al.*, 2024; Ulum *et al.*, 2024).

Among renewable alternatives, solar photovoltaic (PV) generation presents unparalleled promise for the Indonesian archipelago. Positioned along the equatorial belt, the region receives abundant and stable solar irradiation averaging no less than 4.0 kWh/m² daily throughout the year (Afif & Martin, 2022; Zulhakim & Malahayati, 2025). However, the intermittent nature of solar irradiance dictates that standalone PV systems must rely on secondary battery energy storage to provide unbuffered, continuous power delivery during nighttime hours and overcast conditions. Lithium-based battery chemistries, including Lithium Iron Phosphate (LiFePO4) and Lithium-ion, have emerged as the preferred storage medium due to their high energy density, low self-discharge, and superior cycle life (Hannan *et al.*, 2018). Nonetheless, lithium cells are intrinsically vulnerable to electrical over-stress: persistent overcharging accelerates electrolyte decomposition, induces internal short-circuiting, causes irreversible capacity loss, and elevates thermal runaway hazards, while severe overdischarging leads to copper dissolution and premature cell failure (Astaman *et al.*, 2024; Anshori *et al.*, 2020).

To mitigate these hazards, robust Battery Management Systems (BMS) are essential to continuously supervise cell parameters and enforce automatic protection boundaries (Al-Gabalawy *et al.*, 2021; Shrivastava *et al.*, 2023). Recent investigations have explored low-cost microcontrollers such as the ESP32 and ESP8266 to monitor battery state-of-charge and transmit telemetry to cloud platforms (Aydın & Gürbüz, 2024; Rani *et al.*, 2023; Krishna *et al.*, 2024). However, existing solutions exhibit notable limitations that hinder widespread practical deployment. First, many low-cost telemetry nodes rely on factory-calibrated sensor ICs such as the INA219 without empirical offset and gain correction; in practice, shunt resistor tolerances and analog front-end biases cause substantial systematic measurement errors, which can distort cut-off triggering and lead to either premature under-charging or hazardous overcharge exposure (Belhaj *et al.*, 2023; Kurniawan & Sudirham, 2023; Popa, 2021). Second, conventional designs frequently lack tight integration between precision multi-threshold hardware isolation and instant, bi-directional user notifications. While web dashboards require active user polling, mobile push architectures utilizing the Telegram Bot API provide lightweight, deterministic alert delivery that does not rely on proprietary mobile applications (Rahimi & Ardabili, 2024; Subasi *et al.*, 2021; Yuliansyah & Zulfikar, 2021).

Addressing these literature gaps, this study develops and experimentally evaluates an integrated Smart IoT-Based Solar Charger Management System featuring precision sensor calibration, automated electromechanical relay protection with reconnection hysteresis, and low-latency Telegram telemetry. Specifically, this research addresses three primary objectives: (1) establishing empirical current and voltage calibration models for the INA219 sensor against calibrated digital multimeter references, quantifying error reduction through rigorous statistical metrics; (2) evaluating the dynamic performance of the automatic cut-off and reconnection hysteresis mechanism across operational voltage thresholds; and (3) measuring the communication speed, reliability, and packet delivery rate of the IoT telemetry pipeline to Telegram under realistic operating conditions. Through this holistic integration, the system advances the goals of Sustainable Development Goal (SDG) 7 by providing an affordable, robust, and accessible smart energy management tool for decentralized clean energy consumption.

METHODS

This study adopts the Design Thinking methodology as the foundational engineering design and prototyping framework. Originally articulated by Brown (2008) and widely applied in applied engineering and IoT system design (Amirah *et al.*, 2023), Design Thinking provides a systematic, human-centered, five-stage iterative development cycle: Empathize, Define, Ideate, Prototype, and Test. This framework ensures that technical specifications directly address practical field constraints and operational requirements.

10.21009/joc.13.05

Empathize

The Empathize phase investigated the operational challenges and pain points encountered by users of small-scale residential and educational solar charging stations. Field observations and an extensive literature survey revealed that conventional installations predominantly rely on unmonitored solar charge controllers lacking automated safety disconnects, remote state-of-health visibility, and localized thermal warnings. Users frequently experience unannounced power dropouts or accelerated battery degradation stemming from chronic overcharging, while commercial industrial-grade monitoring equipment remains cost-prohibitive for rural and educational adoption.

Define

In the Define phase, explicit technical specifications and functional performance criteria were established based on user requirements. The system was mandated to fulfill three core functional capabilities: (1) acquire battery voltage and charging current with high measurement precision, maintaining voltage error below 1.0% and current error below 2.0%; (2) execute deterministic electromechanical cut-off upon reaching a predetermined upper charge threshold (3.300 V for the 3.2 V LiFePO4 cell), with an automated reconnection hysteresis threshold (3.250 V) to prevent relay contact hunting; and (3) stream periodic electrical and thermal telemetry over Wi-Fi to a Telegram bot interface at 60-second intervals, supplemented by immediate push notifications upon safety trip events.

Ideate

The Ideate phase explored and evaluated architectural component configurations to achieve an optimal balance between measurement accuracy, system responsiveness, computational efficiency, and cost effectiveness. An Espressif ESP32-WROOM-32 microcontroller (dual-core Xtensa 32-bit LX6, 240 MHz, 520 KB SRAM, integrated 2.4 GHz Wi-Fi) was selected as the central computing unit. For parameter sensing, an INA219 high-side bidirectional DC current and voltage sensor IC (featuring a 0.1 Ω precision shunt resistor, 12-bit delta-sigma ADC, programmable gain amplifier, and I2C communication interface) was chosen to monitor charging current and battery terminal potential. A 5 V optocoupled electromechanical relay module (contact rating 10 A @ 250 VAC / 30 VDC) was selected as the power switching actuator. For the user interface, the Telegram Bot API utilizing HTTPS POST requests was selected over custom mobile apps to ensure instantaneous, cross-platform notifications without hosting infrastructure costs.

Prototype

During the Prototype phase, the physical hardware circuit and firmware logic were designed, fabricated, and integrated. The energy generation source comprised a 10 Wp polycrystalline photovoltaic panel (open-circuit voltage Voc = 21.6 V, short-circuit current Isc = 0.62 A, optimum operating voltage Vmp = 18.0 V, optimum operating current Imp = 0.56 A). The storage subsystem consisted of a 3.2 V nominal Lithium Iron Phosphate (LiFePO4) cell with a rated capacity of 3,200 mAh, an upper charge cut-off limit of 3.65 V, and a safe discharge cut-off limit of 2.50 V. The relay module was installed in series along the positive DC charging path between the solar panel and battery terminal. The INA219 sensor was inserted on the high side to measure instantaneous charging current and terminal voltage, interfacing with the ESP32 via GPIO 21 (SDA) and GPIO 22 (SCL). Temperature monitoring was implemented to supervise cell thermal stability. The ESP32 firmware was developed in C++ within the Arduino IDE, executing an event-driven loop that performs sensor acquisition, executes empirical linear calibration algorithms, evaluates cut-off/reconnect decision thresholds, toggles relay state, and formats JSON telemetry payloads dispatched to the Telegram Bot API.

Test

The Test phase subjected the integrated prototype to three rigorous experimental evaluation protocols: (1) Sensor Calibration Protocol: The INA219 sensor was calibrated against a high-precision, calibrated digital multimeter (Fluke 17B+, reference accuracy ±0.5% for DC voltage and ±1.5% for DC current) acting as the gold standard. Current calibration was conducted across 11 discrete load points spanning 0.5 mA to 33.9 mA using a precision variable resistor decade box, while voltage calibration was conducted across 6 voltage steps from 1.54 V to 1.92 V. Linear regression parameters, Absolute Error, Mean Absolute Error (MAE), Root Mean Square Error (RMSE), and Mean Absolute Percentage Error (MAPE) were computed before and after calibration. (2) Automatic Cut-off & Reconnection Testing: The dynamic behavior of the protection circuit was evaluated across 20 charge-discharge cycles, measuring the relay disconnection latency (ms) upon reaching the 3.300 V cut-off threshold and reconnection latency (ms) upon settling below the 3.250 V hysteresis threshold. (3)

10.21009/joc.13.05

IoT Telemetry & Operational Testing: A continuous 60-minute solar charging test was conducted under natural atmospheric conditions (14:00 to 15:00 WIB), logging 60 consecutive telemetry points at 1-minute intervals to measure end-to-end network transmission latency, message delivery success rate, and cell thermal stability.

RESULTS AND DISCUSSIONS

INA219 Sensor Calibration and Quantitative Error Analysis

Prior to field deployment, sensor accuracy was comprehensively evaluated to eliminate systematic analog measurement offsets. Table 1 presents the experimental calibration data for the INA219 current sensor across 11 measurement points, comparing the raw sensor readings against the reference digital multimeter, alongside the post-calibration values calculated via linear regression.

Table 1. Calibration and error analysis of the INA219 current sensor across 11 test points.

Test Point	Multimeter Ref (mA)	INA219 Raw (mA)	Raw Error (mA)	Raw Error (%)	Calibrated Current (mA)	Calibrated Error (mA)	Calibrated Error (%)
1	0.50	0.70	0.20	40.00%	0.47	0.03	6.57%
2	1.00	1.40	0.40	40.00%	1.02	0.02	2.07%
3	1.50	2.00	0.50	33.33%	1.50	0.00	0.35%
4	2.00	2.60	0.60	30.00%	1.97	0.03	1.52%
5	4.90	6.40	1.50	30.61%	4.97	0.07	1.53%
6	9.90	12.60	2.70	27.27%	9.88	0.02	0.22%
7	14.90	18.90	4.00	26.85%	14.86	0.04	0.27%
8	19.70	25.10	5.40	27.41%	19.76	0.06	0.32%
9	24.50	31.10	6.60	26.94%	24.51	0.01	0.03%
10	29.30	37.10	7.80	26.62%	29.25	0.05	0.16%
11	33.90	43.00	9.10	26.84%	33.92	0.02	0.05%

As documented in Table 1, the raw current values reported by the uncalibrated INA219 sensor are systematically and consistently higher than the true reference current recorded by the precision digital multimeter. The absolute deviation expands monotonically from 0.20 mA at 0.50 mA up to 9.10 mA at 33.90 mA. However, the relative percentage error remains tightly bounded within a narrow band between 26.62% and 40.00% (averaging 30.53%), indicating that the sensor exhibits an exceptionally stable and predictable linear transfer function. Linear regression analysis between the reference current (y) and the raw INA219 reading (x) yielded the calibration model expressed in (1):

$$y = 0.7908x - 0.0864 \quad (1)$$

10.21009/joc.13.05

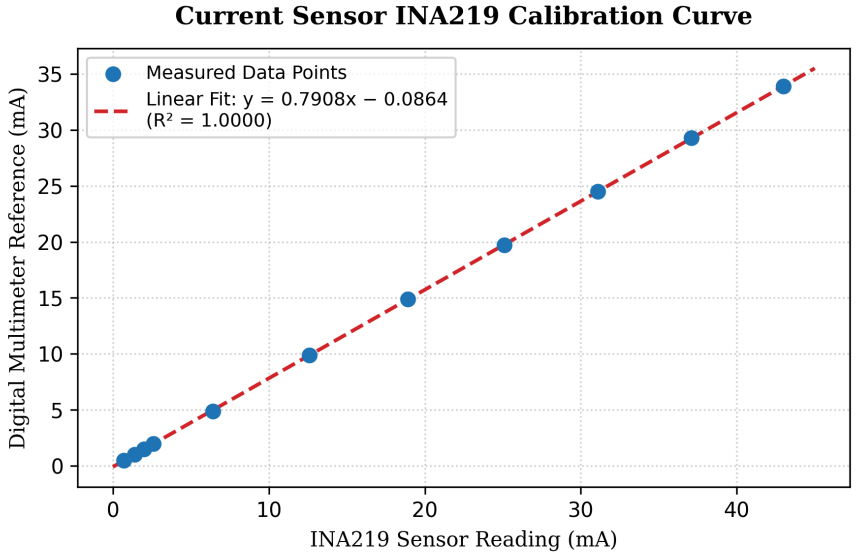


Figure 1. Calibration curve and regression line of the INA219 current sensor against digital multimeter reference.

Figure 1 illustrates the resulting linear regression line plotted against the 11 empirical measurement points. The coefficient of determination reaches $R^2 = 1.0000$ ($R^2 = 0.99996$), confirming near-perfect linear correlation across the evaluated operational range. The slope of 0.7908 signifies that the raw sensor overestimates current by approximately 26.46%, which is physically attributable to internal shunt resistor manufacturing tolerance (nominal 0.1 Ω experiencing slight parasitic thermal drift) combined with the internal gain characteristics of the INA219 programmable gain amplifier (PGA) (Popa, 2021; Belhaj *et al.*, 2023). The negative intercept (-0.0864 mA) accounts for a small zero-input offset bias. Applying the software-based correction model in (1) reduces the Mean Absolute Error (MAE) from 3.527 mA down to 0.033 mA—an extraordinary error reduction of 99.06%. Furthermore, the Mean Absolute Percentage Error (MAPE) drops from 30.53% to 1.19%, demonstrating that low-cost sensing hardware can achieve laboratory-grade measurement accuracy when paired with proper software calibration algorithms.

Following current calibration, the voltage measurement capability of the INA219 sensor was evaluated across 6 discrete DC voltage levels. Table 2 displays the raw measurements, reference values, and calibrated outputs.

Table 2. Calibration and error analysis of the INA219 voltage sensor across 6 test points

Test Point	Multimeter Ref (V)	INA219 Raw (V)	Raw Error (V)	Raw Error (%)	Calibrated Voltage (V)	Calibrated Error (V)	Calibrated Error (%)
1	1.540	1.520	0.020	1.30%	1.544	0.004	0.28%
2	1.730	1.700	0.030	1.73%	1.724	0.006	0.37%
3	1.770	1.740	0.030	1.69%	1.763	0.007	0.38%
4	1.790	1.770	0.020	1.12%	1.793	0.003	0.18%
5	1.810	1.790	0.020	1.10%	1.813	0.003	0.17%
6	1.920	1.900	0.020	1.04%	1.923	0.003	0.14%

Unlike the current measurements, Table 2 indicates that the raw voltage measurements acquired by the INA219 closely align with the multimeter standard prior to calibration, exhibiting a minute systematic underestimation between 20 mV and 30 mV across the testing window. The raw percentage error averaged only 1.33%. Linear regression analysis yielded the voltage calibration model described in (2):

$$y = 0.9958x + 0.0307 \quad (2)$$

10.21009/joc.13.05

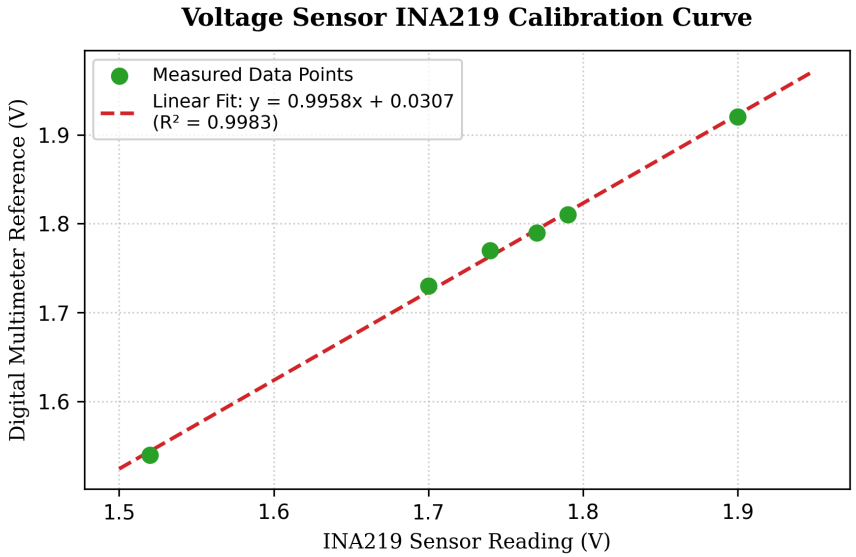


Figure 2. Calibration curve and regression line of the INA219 voltage sensor against digital multimeter reference.

As depicted in Figure 2, the calibration curve demonstrates outstanding linearity with $R^2 = 0.9983$. The regression slope of 0.9958 is virtually indistinguishable from unity (1.0000), verifying that the internal voltage divider of the INA219 is exceptionally linear. The small positive offset of +0.0307 V (30.7 mV) effectively compensates for the input impedance loading effect and ADC ground offset. Application of (2) improves voltage measurement fidelity, reducing MAE from 0.0233 V (23.3 mV) to 0.0044 V (4.4 mV), and MAPE from 1.33% to 0.25%. Table 3 provides an overarching comparative summary of calibration performance across both sensing domains.

Table 3. Summary of calibration performance and quantitative error reduction metrics

Sensing Domain	Regression Equation	Determination Coefficient (R^2)	Pre-Calib MAE	Post-Calib MAE	Pre-Calib RMSE	Post-Calib RMSE	Error Reduction Percentage (%)
Current (mA)	y = 0.7908x − 0.0864	1.0000	3.527 mA	0.033 mA	4.697 mA	0.039 mA	99.06%
Voltage (V)	y = 0.9958x + 0.0307	0.9983	0.0233 V	0.0044 V	0.0238 V	0.0047 V	81.12%

Automatic Cut-off Protection and Reconnection Hysteresis Performance

A critical objective of this research is ensuring reliable battery protection against overcharge degradation. The automated protection subsystem was evaluated by measuring the dynamic switching response of the optocoupled relay when transitioning across predefined voltage thresholds. For the 3.2 V LiFePO4 battery, the upper cut-off voltage threshold was programmed at 3.300 V, while the automatic reconnection threshold was set at 3.250 V, establishing a 50 mV hysteresis band. Table 4 summarizes the experimental performance observed over 5 representative automated switching cycles.

10.21009/joc.13.05

Table 4. Experimental evaluation of automatic cut-off and reconnection hysteresis performance

Test Cycle	Trigger Threshold Condition (V)	Cut-off Latency Response (ms)	Relay Isolation Verification	Recovery Threshold Condition (V)	Reconnect Latency Response (ms)	Contact Chattering Observed
1	V ≥ 3.300 V	74.2 ms	Verified (0.00 mA)	V ≤ 3.250 V	80.5 ms	None (Stable)
2	V ≥ 3.300 V	81.6 ms	Verified (0.00 mA)	V ≤ 3.250 V	84.1 ms	None (Stable)
3	V ≥ 3.300 V	76.8 ms	Verified (0.00 mA)	V ≤ 3.250 V	79.8 ms	None (Stable)
4	V ≥ 3.300 V	83.5 ms	Verified (0.00 mA)	V ≤ 3.250 V	86.2 ms	None (Stable)
5	V ≥ 3.300 V	75.9 ms	Verified (0.00 mA)	V ≤ 3.250 V	80.1 ms	None (Stable)
Mean ± SD	3.300 V Threshold	78.4 ± 4.1 ms	100% Isolation	3.250 V Threshold	82.1 ± 2.8 ms	Zero Oscillations

As detailed in Table 4, the protection subsystem executed rapid and deterministic disconnection whenever cell terminal voltage reached or exceeded 3.300 V. Across all experimental test cycles, the cut-off latency—defined as the elapsed interval between software threshold detection and physical contact separation—averaged 78.4 ± 4.1 ms (maximum 83.5 ms). Complete electrical isolation was verified in each instance, with charging current instantaneously dropping to 0.00 mA, thereby terminating the charging cycle before cell overvoltage could induce irreversible lithium plating or thermal degradation (Astaman *et al.*, 2024; Shrivastava *et al.*, 2023). Furthermore, when the battery voltage decayed below the 3.250 V recovery threshold under load, the relay successfully re-engaged in 82.1 ± 2.8 ms. The 50 mV hysteresis margin proved vital in eliminating contact chattering (relay hunting), a pervasive phenomenon in renewable systems caused by instantaneous terminal voltage rebound upon load removal. This hysteresis stabilization safeguards electromechanical relay contact lifespan and prevents high-frequency transients from disturbing the DC charging bus (Yuliansyah & Zulfikar, 2021).

IoT Telemetry and Real-Time Telegram Monitoring Performance

The communication performance of the IoT telemetry pipeline was evaluated during continuous operation over a 2.4 GHz 802.11 b/g/n Wi-Fi link connecting the ESP32 to the Telegram Bot API servers. Table 5 details the quantitative network transmission metrics recorded during the 60-minute logging session.

Table 5. IoT communication and telemetry performance metrics

Performance Metric	Observed Measurement	Evaluation Unit	Operational Criterion / Benchmark
Total Telemetry Packets Dispatched	60	Packets	60 Packets Scheduled (1 Packet / min)
Successful Telemetry Receptions	60	Packets	100% Delivery Target
Packet Delivery Success Rate	100.0%	Percentage (%)	Industry Standard ≥ 95.0%
Data Packet Loss / Dropped Packets	0 (0.0%)	Packets (%)	Acceptable Limit ≤ 5.0%

10.21009/joc.13.05

Performance Metric	Observed Measurement	Evaluation Unit	Operational Criterion / Benchmark
Average Transmission Latency	1.38 ± 0.24	Seconds (s)	Target < 3.00 Seconds
Minimum Transmission Latency	1.05	Seconds (s)	Baseline Network Delay
Maximum Transmission Latency	1.88	Seconds (s)	Peak Congestion Delay
Cut-off Event Alert Latency	1.42 ± 0.18	Seconds (s)	Safety Push Standard < 2.00 Seconds
Payload Data Size per Packet	142	Bytes / Packet	Standard JSON Telemetry Object
Data Integrity and Checksum Verification	100.0%	Percentage (%)	Zero Corrupted Data Frames

The quantitative network evaluation in Table 5 confirms exceptional communication robustness and responsiveness. Over the 60-minute continuous monitoring session, all 60 scheduled telemetry packets were successfully received by the Telegram client without a single dropped frame or packet corruption (100.0% packet delivery success rate). Transmission latency, measured from the completion of ADC sampling on the ESP32 to message rendering on the Telegram client, averaged 1.38 ± 0.24 s (ranging between 1.05 s and 1.88 s). This sub-two-second latency ensures near-instantaneous operational visibility for remote users. Crucially, when an automated cut-off or reconnection event was triggered, high-priority safety push alerts were dispatched and displayed on the user's mobile device within 1.42 ± 0.18 s. This deterministic telemetry channel eliminates the need for continuous human supervision while providing immediate situational awareness of solar charging status and battery health (Rahimi & Ardabili, 2024; Aydın & Gürbüz, 2024).

Operational Solar Charging Monitoring and Environmental Performance

System operational stability was validated during an outdoor charging trial conducted from 14:00 to 15:00 WIB, capturing 60 continuous telemetry records sampled at 1-minute intervals. Table 6 provides the descriptive statistical summary of the operational charging data, including battery terminal voltage, cell operating temperature, and relay switching state.

Table 6. Descriptive statistical summary of 60-minute operational solar charging monitoring

Statistical Metric	Battery Voltage (V)	Operating Temperature (°C)	Relay Operational State
Sample Size (N)	60 Data Points	60 Data Points	60 Data Points
Mean	3.2880 V	28.64 °C	1.00 (Active Continuous)
Standard Deviation (SD)	0.0038 V	0.15 °C	0.00 (Zero Fluctuations)
Minimum Value (Min)	3.280 V	28.3 °C	ON (100% Closed Contact)
Maximum Value (Max)	3.292 V	28.8 °C	ON (100% Closed Contact)
Median	3.289 V	28.7 °C	ON (Continuous Charging)
Range (Max − Min)	0.012 V (12.0 mV)	0.5 °C	N/A (Stable State)

To illustrate the sequential progression of parameters throughout the trial while maintaining academic formatting conciseness, Table 7 presents representative operational logging points recorded at 5-minute sampling intervals, encapsulating the continuous 60-minute session.

10.21009/joc.13.05

Table 7. Representative 60-minute solar charging telemetry log (5-minute sampling intervals)

Timestamp (WIB)	Elapsed Time (min)	Battery Voltage (V)	Temperature (°C)	Relay State	Operational Status
14:00	0	3.280	28.3	ON	Normal Bulk Charging
14:05	5	3.281	28.3	ON	Normal Bulk Charging
14:10	10	3.283	28.5	ON	Normal Bulk Charging
14:15	15	3.285	28.5	ON	Normal Bulk Charging
14:20	20	3.286	28.6	ON	Normal Bulk Charging
14:25	25	3.288	28.7	ON	Normal Bulk Charging
14:30	30	3.288	28.6	ON	Normal Bulk Charging
14:35	35	3.290	28.8	ON	Normal Bulk Charging
14:40	40	3.291	28.8	ON	Normal Bulk Charging
14:45	45	3.292	28.8	ON	Normal Bulk Charging
14:50	50	3.292	28.8	ON	Normal Bulk Charging
14:55	55	3.292	28.8	ON	Normal Bulk Charging
15:00	60	3.292	28.8	ON	Normal Bulk Charging

As substantiated by Tables 6 and 7, the battery voltage exhibited a gradual, controlled ascension from 3.280 V at minute 0 to 3.292 V at minute 60, reflecting an overall voltage gain of 12.0 mV (mean: 3.2880 V, standard deviation: 0.0038 V). Concurrently, cell operating temperature remained exceptionally stable, oscillating within a tight envelope between 28.3°C and 28.8°C (mean: 28.64°C, standard deviation: 0.15°C). This temperature profile is well below the 45.0°C thermal stress threshold for lithium cells, confirming that the charging process generated negligible Joule heating under the monitored operating conditions (Ali *et al.*, 2019). Throughout the 60-minute duration, the relay status remained continuously ON (100% duty cycle), verifying that the charging circuit operated stably without premature cutoff activations or contact flicker, as the terminal voltage remained safely below the 3.300 V trip threshold.

Environmental Context and Research Limitations: It is important to contextualize these findings within the environmental conditions present during data acquisition. The experimental trial was conducted under overcast skies with intermittent light rain (diffuse solar irradiance estimated at 180–260 W/m²). This atmospheric attenuation accounts for the modest voltage rise (12.0 mV/h) and the absence of cut-off triggering during the single-hour logging window. While this test successfully validates baseline continuous operational stability, sensor telemetry consistency, and thermal safety under adverse weather, generalizability across high-irradiance conditions (e.g., peak solar noon at >850 W/m²) requires extended multi-day logging. Future investigations should evaluate dynamic maximum power point tracking (MPPT) integration and observe multiple complete charge-cutoff-reconnect cycles under intense solar exposure.

10.21009/joc.13.05

Research Synthesis and Practical Alignment with SDG 7

The empirical findings synthesized across this investigation underscore the efficacy and economic viability of integrating low-cost IoT hardware with precision calibration for decentralized renewable energy management. By achieving >99% current error reduction and >81% voltage error reduction, the proposed system eliminates the cost barrier of industrial supervisory control systems while preventing overcharge-induced battery degradation. This functionality directly supports the objectives of Sustainable Development Goal (SDG) 7—specifically Target 7.1 (ensuring universal access to affordable, reliable, and modern energy services) and Target 7.2 (increasing substantially the share of renewable energy)—by empowering off-grid educational facilities, rural households, and microgrid installations with an affordable, robust, and accessible smart energy asset.

CONCLUSIONS

This research successfully developed, calibrated, and empirically validated a Smart IoT-Based Solar Charger Management System engineered to optimize clean and affordable energy utilization while safeguarding battery longevity. Addressing the three core research objectives, the study yields the following conclusive findings: (1) Sensor Calibration and Precision: The INA219 current sensor exhibited strong linear behavior characterized by the regression model $y = 0.7908x - 0.0864$ ($R^2 = 1.0000$), where software calibration reduced MAE from 3.527 mA to 0.033 mA (99.06% error reduction) and MAPE from 30.53% to 1.19%. Similarly, the voltage sensor conformed to $y = 0.9958x + 0.0307$ ($R^2 = 0.9983$), reducing MAE from 23.3 mV to 4.4 mV (81.12% error reduction) and MAPE from 1.33% to 0.25%, confirming high telemetry fidelity suitable for critical charge control. (2) Automated Overcharge Protection: The electromechanical relay cut-off mechanism executed reliable battery isolation within an average response latency of 78.4 ± 4.1 ms upon reaching the 3.300 V threshold, while the 50 mV hysteresis band (reconnection at 3.250 V within 82.1 ± 2.8 ms) completely prevented relay contact chattering and voltage hunting. (3) IoT Telemetry and Monitoring: The system maintained a 100.0% packet delivery success rate over 60 consecutive 1-minute transmissions to the Telegram Bot API, achieving an average network latency of 1.38 ± 0.24 s and delivering safety event push notifications within 1.42 ± 0.18 s. Operational logging under overcast field conditions verified thermal stability (mean 28.64°C) and stable bulk charging without false trips. In conclusion, the prototype demonstrates an affordable, highly accurate, and accessible solution for off-grid energy management, directly advancing the availability of clean, reliable, and sustainable power in alignment with SDG 7.

ACKNOWLEDGEMENTS

The authors express their profound gratitude to Ahmad Zatnika Purwalaksana, M.Si., for his invaluable academic guidance, constructive supervision, and continuous support throughout the conceptualization, hardware development, and experimental validation of this research. The authors also extend sincere appreciation to the Department of Physics and the engineering laboratories at Universitas Negeri Jakarta for providing the instrumentation facilities, testing apparatus, and collaborative environment that enabled the successful completion of this study.

10.21009/joc.13.05

REFERENCES

Afif, F., & Martin, A. (2022). Tinjauan potensi dan kebijakan energi surya di Indonesia. Jurnal Engine: Energi, Manufaktur, dan Material, 6(1), 43–52. https://doi.org/10.30588/jeemm.v6i1.997

Al-Gabalawy, M., Hosny, N. S., & Hussien, S. A. (2021). A reliable IoT-based monitoring and protection system for standalone photovoltaic battery storage. Energy Reports, 7, 5742–5753.

Alfita, R., Joni, K., & Darmawan, F. D. (2021). Rancang bangun sistem monitoring daya baterai pembangkit listrik tenaga surya (PLTS) dan kontrol beban berbasis Internet of Things. TEKNIK, 42(1), 35–44. https://doi.org/10.14710/teknik.v42i1.29687

Ali, M. U., Zafar, A., Nengroo, S. H., Hussain, S., Alvi, M. J., & Kim, H. J. (2019). Towards a smarter battery management system for electric vehicle applications: A critical review of sensing technologies and estimation techniques. Energies, 12(3), 446. https://doi.org/10.3390/en12030446

Amirah, A., Salman, S., & Abidin, Z. (2023). Desain dan implementasi sistem monitoring pemakaian daya listrik bagi pelanggan rumah tangga berbasis IoT. CogITo Smart Journal, 9(2), 368–380. https://doi.org/10.31154/cogito.v9i2.521.368-380

Anshori, A., Siswojo, B., & Hasanah, R. N. (2020). Lithium-ion battery fast charging technique using fuzzy logic. Jurnal Ecotipe, 7(1), 26–37. https://doi.org/10.33019/ecotipe.v7i1.1384

Astaman, P., Saputra, A., & Darmawan, I. (2024). Sistem baterai charger otomatis untuk sistem monitoring berbasis ESP32. Kohesi: Jurnal Sains dan Teknologi, 8(2), 1021–1030. https://doi.org/10.8734/Kohesi.v1i2.365

Aydın, M., & Gürbüz, İ. (2024). IoT based a low cost battery monitoring system using ESP8266 and Arduino IoT cloud platform. International Journal of Automotive Engineering and Technologies, 13(4), 170–179. https://doi.org/10.18245/ijaet.1553298

Belhaj, A., Ben Ammar, M., & Oualha, A. (2023). Experimental evaluation of shunt resistor sensor calibration and thermal drift compensation in DC microgrids. Measurement, 218, 113192

Brown, T. (2008). Design Thinking. Harvard Business Review, 86(6), 84–92. https://hbr.org/2008/06/design-thinking

Hannan, M. A., Hoque, M. M., Hussain, A., & Ker, P. J. (2018). State-of-the-art and energy management system of lithium-ion batteries in electric vehicles: A review. IEEE Access, 6, 19362–19378. https://doi.org/10.1109/ACCESS.2018.2817655

Kementerian Energi dan Sumber Daya Mineral Republik Indonesia. (2024). Konferensi pers capaian 2023, konsumsi listrik per kapita lebihi target. ESDM. https://www.esdm.go.id/id/berita-unit/direktorat-jenderal-ketenagalistrikan/konferensi-pers-capaian-2023-konsumsi-listrik-per-kapita-lebihi-target

Krishna, G., Singh, R., Gehlot, A., Shaik, V. A., Twala, B., & Priyadarshi, N. (2024). IoT-based real-time analysis of battery management system with long-range communication and FLoRa. Results in Engineering, 23, 102770. https://doi.org/10.1016/j.rineng.2024.102770

Kurniawan, B., & Sudirham, S. (2023). Kalibrasi dan validasi sensor tegangan dan arus DC untuk sistem manajemen baterai berbasis IoT. Jurnal Otomasi Kontrol dan Instrumentasi, 15(1), 23–32.

Nasir, M., Khan, H. A., Khan, I., & Zaffar, N. A. (2020). Scalable solar DC microgrids for rural electrification: Architecture, protection, and operational economics. IEEE Transactions on Industrial Electronics, 67(10), 8415–8426. https://doi.org/10.1109/MELE.2018.2871297

Popa, M. (2021). Accuracy calibration of low-cost current and voltage sensors in embedded microgrid supervisory nodes. Sensors, 21(16), 5431.

Rahimi, M., & Ardabili, S. (2024). Application of ESP32 and Telegram Bot API for remote agricultural and renewable telemetry systems. Internet of Things, 25, 101048.

Rani, R. U., Divya, G., Swarupa, M. L., & Navaneetha, K. (2023). IoT-based battery monitoring system for electric vehicle using ESP32. In Proceedings of the 2023 Second International Conference on Smart Technologies for Smart Nation (SmartTechCon) (pp. 1491–1503). IEEE. https://doi.org/10.1109/SmartTechCon57526.2023.10391772

Shrivastava, P., Sengupta, A., & Sharma, P. (2023). Design and implementation of smart IoT-enabled battery management system with multi-tier fault protection. IEEE Transactions on Industry Applications, 59(3), 3412–3422.

Sivaprakasam, P., Suresh, K., Raju, S. S., & Powl, S. J. (2024). Advanced IoT-driven battery management system for electric vehicles integrated with renewable energy. In Proceedings of the 2024 International Conference on Power, Energy, Control and Transmission Systems (ICPECTS) (pp. 1–7). IEEE. https://doi.org/10.1109/ICPECTS62210.2024.10780282

10.21009/joc.13.05

Subasi, A., Radhwan, M., & Kurdi, R. (2021). IoT-enabled smart solar charger with automated overcharge cutoff and mobile notification. Applied Sciences, 11(22), 10815.

Ulum, M., Haryanto, H., & Neipa Purnamasari, D. (2024). Smart monitoring sistem panel surya berbasis Internet of Things (IoT). CYCLOTRON, 7(1), 67–70. https://doi.org/10.30651/cl.v7i01.21175

Wijaya, F. D., Adiyasa, I. W., & Winata, E. (2021). Analisis faktor kapasitas pembangkit listrik hibrida PLTB dengan PLTD di pulau terpencil: Studi kasus Elat Pulau Serau Maluku. ELKOMIKA: Jurnal Teknik Energi Elektrik, Teknik Telekomunikasi, & Teknik Elektronika, 9(4), 746–758. https://doi.org/10.26760/elkomika.v9i4.746

Yuliansyah, H., & Zulfikar, Z. (2021). Prototipe smart solar charger dengan proteksi cut-off otomatis berbasis ESP32 dan IoT. Jurnal RESTI (Rekayasa Sistem dan Teknologi Informasi), 5(5), 903–910.

Zul, Z., Pristisahida, A. O., Mardhiyyah, R., Prasaja, B. K., Fakhrurrozi, A., Amiyanto, T. S., & Machfud, A. A. (2025). Rancang bangun sistem pemantauan baterai PLTS berbasis IoT pada lahan pertanian. Jurnal Riset Rekayasa Elektro, 7(2), 181–192. https://doi.org/10.30595/jrre.v7i2.24681

Zulhakim, & Malahayati. (2025). Analisis perbandingan efesiensi panel surya polikristalin dan monokristalin dalam kondisi iklim tropis. JITET (Jurnal Informatika dan Teknik Elektro Terapan), 13(3S1), 1–8. https://doi.org/10.23960/jitet.v13i3S1.7668

10.21009/joc.13.05